

# Isometric and isovelocity contractile performance of red muscle fibres from the dogfish *Scyliorhinus canicula*

F. Lou<sup>1,\*</sup>, N. A. Curtin<sup>1,†</sup> and R. C. Woledge<sup>2</sup>

<sup>1</sup>Biological Structure and Function, Division of Biomedical Sciences, Faculty of Medicine, Sir Alexander Fleming Building, Imperial College of Science, Technology and Medicine, London SW7 2AZ and <sup>2</sup>UCL Institute of Human Performance, Royal National Orthopaedic Hospital Trust, Brockley Hill, Stanmore, Middlesex HA7 4LP, UK

\*Present address: Department of Biosciences, Faculty of Natural Sciences, University of Hertfordshire, College Lane, Hatfield, Hertfordshire AL10 9AB, UK

†Author for correspondence (e-mail: n.curtin@ic.ac.uk)

Accepted 19 March 2002

## Summary

Maximum isometric tetanic force produced by bundles of red muscle fibres from dogfish, *Scyliorhinus canicula* (L.), was  $142.4 \pm 10.3 \text{ kN m}^{-2}$  ( $N=35$  fibre bundles); this was significantly less than that produced by white fibres  $289.2 \pm 8.4 \text{ kN m}^{-2}$  ( $N=25$  fibre bundles) (means  $\pm$  S.E.M.). Part, but not all, of the difference is due to mitochondrial content. The maximum unloaded shortening velocity,  $1.693 \pm 0.108 L_0 \text{ s}^{-1}$  ( $N=6$  fibre bundles), was measured by the slack-test method.  $L_0$  is the length giving maximum isometric force. The force/velocity relationship was investigated using a step-and-ramp protocol in seven red fibre bundles. The following equation was fitted to the data:  $[(P/P_0) + (a/P_0)](V+b) = [(P_0^*/P_0) + (a/P_0)]b$ , where  $P$  is force during shortening at velocity  $V$ ,  $P_0$  is the isometric force before shortening, and  $a$ ,  $b$  and  $P_0^*$  are fitted constants. The fitted values were  $P_0^*/P_0 = 1.228 \pm 0.053$ ,  $V_{\max} = 1.814 \pm 0.071 L_0 \text{ s}^{-1}$ ,  $a/P_0 = 0.269 \pm 0.024$  and  $b = 0.404 \pm 0.041 L_0 \text{ s}^{-1}$  ( $N=7$  for all values). The maximum power was  $0.107 \pm 0.005 P_0 V_{\max}$  and was produced during

shortening at  $0.297 \pm 0.012 V_{\max}$ . Compared with white fibres from dogfish, the red fibres have a lower  $P_0$  (49 %) and  $V_{\max}$  (48 %), but the shapes of the force/velocity curves are similar. Thus, the white and red fibres have equal capacities to produce power within the limits set by the isometric force and maximum velocity of shortening of each fibre type. A step shortening of  $0.050 \pm 0.003 L_0$  ( $N=7$ ) reduced the maximum isometric force in the red fibres' series elasticity to zero. The series elasticity includes all elastic structures acting in series with the attached cross-bridges. Three red fibre bundles were stretched at a constant velocity, and force (measured when length reached  $L_0$ ) was  $1.519 \pm 0.032 P_0$ . In the range of velocities used here,  $-0.28$  to  $-0.63 V_{\max}$ , force varied little with the velocity.

Key words: red muscle, fish, muscle, contraction, power, isometric force,  $P_0$ , force/velocity, force, series elasticity,  $V_0$ ,  $V_{\max}$ , *Scyliorhinus canicula*, dogfish.

## Introduction

Dogfish myotomal muscle consists of three fibre types, white, red and superficial. In common with teleost fish, the different types are well segregated in the body. The white fibres make up the bulk of the body, the red fibres form a band along the lateral edge of the body and the single layer of superficial fibres is confined to a narrow band between the skin and the red fibres. Each fibre type has a distinct histological and biochemical profile which, at least for white and red fibres, seems well matched to its function during swimming. White fibres are large, with low mitochondrial density and a relatively high glycogen content. They are active during vigorous swimming, which reduces their glycogen content. During sustained slow swimming, the white fibres are not active, and the glycogen content of white fibres does not fall. In contrast, red fibres are small, with high mitochondrial density and relatively high fat content, which falls during their activity in

long periods of sustained swimming (Bone, 1966; Bone et al., 1986).

In this study, two questions are addressed about the contractile performance of red fibres from dogfish. Are they as strong as white fibres during isometric contraction? How much force is produced during constant-velocity movement (shortening and lengthening) at full activation?

Red fibres are small and held together by extensive connective tissue; consequently, some are damaged during dissection of the small bundles of fibres required for *in vitro* experiments. Thus, to answer the question about strength accurately, force must be expressed relative to the cross-sectional area of undamaged fibres. A simple method for identifying damaged and intact fibres has been developed, and quantitative validation of the method is reported.

The mechanical and energetic performance of red fibres

during a brief period of sinusoidal movement have also been investigated (Curtin and Woledge, 1993b). In these 'work-loop' contractions, which are like those that power swimming, the stimulation is brief and not long enough to activate the fibres fully. Here, we report the mechanical properties of fully active red fibres during constant-velocity shortening and lengthening. Although we recognize that these contractions are unlike those powering swimming, they are of value. They give direct information about contractile performance under conditions in which the cross-bridges are not limited or influenced by variations in activation (proportion of cross-bridges that are cycling, etc.). In other words, under conditions in which all variations in force and movement are due solely to cross-bridge properties and none is due to changes in the degree of activation. As we have demonstrated for white fibres, force and power during work loops that mimic swim-like contractions can be predicted by taking account of the behaviour of cross-bridges and the series elasticity (from experiments such as those reported here) and a reasonable assumption about the time course of activation (Curtin et al., 1998).

### Materials and methods

Bundles of red fibres from myotomal muscle were dissected from dogfish, *Scyliorhinus canicula* (L.). The fish were supplied by the Marine Biological Association (Plymouth, UK) and kept in circulating artificial sea water (density 1.26 g ml<sup>-1</sup>) at approximately 12 °C for at least several days before use. Bundles of fibres were dissected from myotomal muscle in the region 0–4 cm caudal to the cloaca. The elasmobranch saline contained (in mmol l<sup>-1</sup>): NaCl, 292; KCl, 3.2; CaCl<sub>2</sub>, 5.0; MgSO<sub>4</sub>, 1.0; Na<sub>2</sub>SO<sub>4</sub>, 1.6; urea, 483; and tubocurarine, 1.5 mg l<sup>-1</sup>. The pH buffer in the saline was NaHCO<sub>3</sub>, equilibrated with air for white fibres, and 5.0 mmol l<sup>-1</sup> Hepes, equilibrated with oxygen, for red fibres. The fibre bundles were immersed in saline during dissection and during the experiments.

### Histology of red fibre bundles

Nine bundles of red fibres were dissected from three fish and stained with 0.005 % Evans Blue, but without any stimulation. After staining and a rinse in saline, these fibre bundles were prepared for cryostat sectioning. The preparation was mounted in gelatine (15 % w/v in saline) while the myosepta were held in forceps to keep the fibres as straight as possible while the gelatine set. After hardening in the refrigerator, the gelatine blocks were trimmed and fixed to cork discs with OCT embedding compound (Histological Equipment Ltd, UK). The blocks were frozen by immersion in partially frozen isopentane for 10 s and stored at -40 °C. Transverse sections of 10 µm thickness were cut on a cryostat (Bright Instrument Company, UK) at -18 °C. Sections were taken at various points along the length of each fibre bundle. They were placed on microscope slides and covered with glycerol and a coverslip.

The sections were examined under a fluorescent microscope

(Olympus Provis) using a green filter that made the Evans-Blue-stained fibres appear bright red and unstained fibres appear dark. Images were recorded and measured with a Photonic Science Olympus video camera operated by the program PhotoLite (Image-Pro). A graticule slide (Graticules Ltd, Kent, England) was recorded and measured in the same series to give the calibration scale.

### Contractile properties

In the experiments on contractile properties, the myosepta at the ends of the fibre bundle were held in T-shaped platinum foil clips. The preparation was mounted in a Perspex bath between a combined motor and force transducer (Cambridge Technology, Inc., model 300B) and a fixed hook. The saline was circulated continuously through the bath and was maintained at approximately 12 °C. The muscle fibre bundle was electrically stimulated (Digitimer, MultiStim System-D330) from end to end through the platinum clips. A program written in TestPoint (Keithley Instruments, UK) controlled stimulation and motor arm position and recorded force, length and stimulation. A DAS-1800AO Series A/D board (Keithley Instruments, UK) was used.

The relationship between force and stimulus strength during tetanic stimulation was investigated in each fibre bundle to establish the supra-maximal stimulus strength. For red fibres, the stimulus strength was varied by changing both the duration (range 0.5–8 ms) and the voltage (0–6 V) of the stimulus pulses. Some fibre bundles produced two responses to stimulation. The first, faster response was produced by every fibre bundle and was the object of interest here. The later response was much slower to develop and could last well over a minute. Increasing stimulus strength by increasing pulse duration rather than voltage was usually effective at producing maximal fast responses, without eliciting a slow response also. The fibre bundle was discarded if a slow response was produced with all stimulus conditions. For white fibres, pulse duration was always brief (0.2 or 0.5 ms), and stimulus strength was varied by changing stimulus voltage. The length/tension relationship was investigated in each fibre bundle to identify the fibre length ( $L_0$ ) at which tetanic force was maximal.

At the end of the experiment, the fibre length at  $L_0$  was measured under a dissecting microscope. Red fibre bundles were stained with Evans Blue, which does not cross intact surface membranes, to distinguish intact from damaged fibres. Bundles were stained with 0.005 % Evans Blue in dogfish saline overnight, then rinsed in saline and transferred to 100 % alcohol for 20 min and then to 5 % formaldehyde. The stained fibres were removed and discarded, and the others were dried and weighed on a Cahn microbalance. White fibre bundles were fixed in alcohol, and damaged fibres, which can be identified without staining, and non-fibre material were removed before the intact fibres were dried and weighed. The cross-sectional area (CSA) was calculated as:

$$CSA = (4.9M/d)/L_0, \quad (1)$$

where  $M$  is dry mass (in mg), 4.9 is the wet-to-dry mass ratio

(Curtin and Woledge, 1993a),  $d$  is density (assumed to be  $1 \text{ mg mm}^{-3}$ ) and  $L_0$  is fibre length (in mm) at which maximum isometric force was produced.

The sarcomere length in red fibres at  $L_0$  was  $2.32 \pm 0.02 \mu\text{m}$  (mean  $\pm$  S.E.M.,  $N=8$  fibres from two fibre bundles from different fish) as measured by laser diffraction.

#### *Red and white fibres: maximum isometric force*

The maximum force,  $P_0$ , during a tetanus at  $L_0$  was measured in purely isometric experiments on 35 bundles of red fibres from 17 fish and 25 bundles of white fibres from 13 fish. The tetanus duration was sufficient for force to reach a plateau value (of at least 0.4 s), indicating that the fibres had been stimulated long enough to become fully active. The stimulation frequency was 29.5 Hz for the red fibre bundles and within the range 25–35 Hz for the white fibre bundles; these frequencies gave fused, maximal tetanic force. The stimulus pulse duration was within the range 1.5–4 ms for red fibres (see above) and was 0.2 ms for white fibres.

#### *$V_0$ for red fibres*

The slack test method (Edman, 1979) was used to determine the shortening velocity at zero load ( $V_0$ ). The muscle preparation was released by different distances ( $\Delta L$ ) from the plateau of an isometric tetanic contraction at  $L_0$  (see Fig. 4A). Regression lines were fitted to the early part of force redevelopment, and the time interval ( $\Delta t$ ) from the release to the start of force redevelopment was measured (see Fig. 4C). The slope of the regression line of  $\Delta L$  versus  $\Delta t$  gives  $V_0$  (see Fig. 4D).

#### *Force/velocity experiments on red fibres*

The muscle fibres were stimulated tetanically at approximately 29.5 Hz every 5 min. For the experiments on both shortening and stretch, movement started during the plateau of the tetanus (0.75 s after the beginning of stimulation). In experiments on shortening, the muscle was released from  $L_0$  by a step reduction in length (0.02–0.2 mm complete in 2 ms) followed by a constant-velocity ramp shortening (at  $1\text{--}8 \text{ mm s}^{-1}$ ). The size of the step was adjusted so that the force remained constant during the first part of the ramp shortening. The duration of tetanus (1.8–3 s) was set so that stimulation continued after the end of shortening. In experiments on stretch, the fibre bundle was stretched at a constant velocity starting from a length less than  $L_0$ ; force was measured when length reached  $L_0$ . Control recordings were made of passive force during movement without stimulation. The control recording was subtracted from the total force recorded during stimulation to give the active force.

#### *Curve-fitting for shortening*

The following equation was used to fit the force/velocity data for shortening for each muscle bundle:

$$[(P/P_0) + (a/P_0)](V + b) = [(P_0^*/P_0) + (a/P_0)]b, \quad (2)$$

where  $P$  is force during shortening at velocity  $V$  ( $L_0 \text{ s}^{-1}$ ),  $P_0$  is

the isometric force before shortening, and  $a$ ,  $b$  and  $P_0^*$  are constants.  $P$ ,  $P_0$  and  $V$  were measured, and the values of the constants  $a$ ,  $b$  and  $P_0^*$  were adjusted to obtain the best fit using Excel Solver. The value of  $V_0$  from the slack test was included in the data to be fitted, but the isometric force,  $P_0$ , was not included.

#### *Characteristics of the series elastic component in red fibre bundles*

The recordings of force during step-and-ramp shortening in force/velocity experiments were also analyzed to give the stress/strain characteristics of the series elastic component of the fibre bundles. The analysis was based on A. V. Hill's (1938) two-component model of muscle consisting of a contractile element, in which force depends on the velocity of movement, and an elastic component in series (SEC) with the contractile component. The force in the SEC is assumed to be dependent on the length of the SEC and to be independent of velocity (Curtin et al., 1998). The step size that is followed by a constant force during subsequent ramp shortening was measured and plotted versus force during shortening to give the strain versus stress relationship of the series elasticity.

#### *Curve-fitting*

The following relationship was fitted to the data points. Strain,  $Y$ , is the sum of a constant,  $k$ , a linear component,  $a(x)$ , and a saturating component,  $b(x)$ , where  $x$  is stress (see Fig. 7A):

$$Y = k + a(x) + b(x), \quad (3)$$

where  $a(x)=mx$ ; if  $x < c$ , then  $b(x)=nx$ ; if  $x \geq c$ , then  $b(x)=nc$ . The Excel Solver function was used to fit values for  $k$ ,  $m$ ,  $n$  and  $c$ .

#### *Statistical analyses*

Values reported are means  $\pm$  S.E.M. and the number of observations is listed.

## **Results**

#### *Red fibre bundles: size and proportion of undamaged fibres*

Fig. 1A shows an example of a transverse cryostat section of a red fibre bundle stained with Evans Blue; the pale fibres in this image are stained damaged fibres, and the grey fibres are those with intact sarcolemmas, which excluded the stain from the intracellular space. Fig. 1B shows a histogram of the cross-sectional areas of the individual intact and damaged fibres in this section. Histograms were produced for each of the sections ( $N=19$ ), and the median area for a live fibre was  $0.00529 \pm 0.00039 \text{ mm}^2$ , which is equivalent to a diameter of  $81.1 \pm 2.9 \mu\text{m}$  assuming a circular cross section. Intact fibres constituted on average  $68.6 \pm 1.8\%$  of the total fibre area in bundles with a total area of  $0.843 \pm 0.055 \text{ mm}^2$ .

Our impression during dissection was that fibres on the surface of the bundle were easily damaged because they are of small diameter and held together tightly by connective tissue. The image in Fig. 1A gives some support for this idea in that

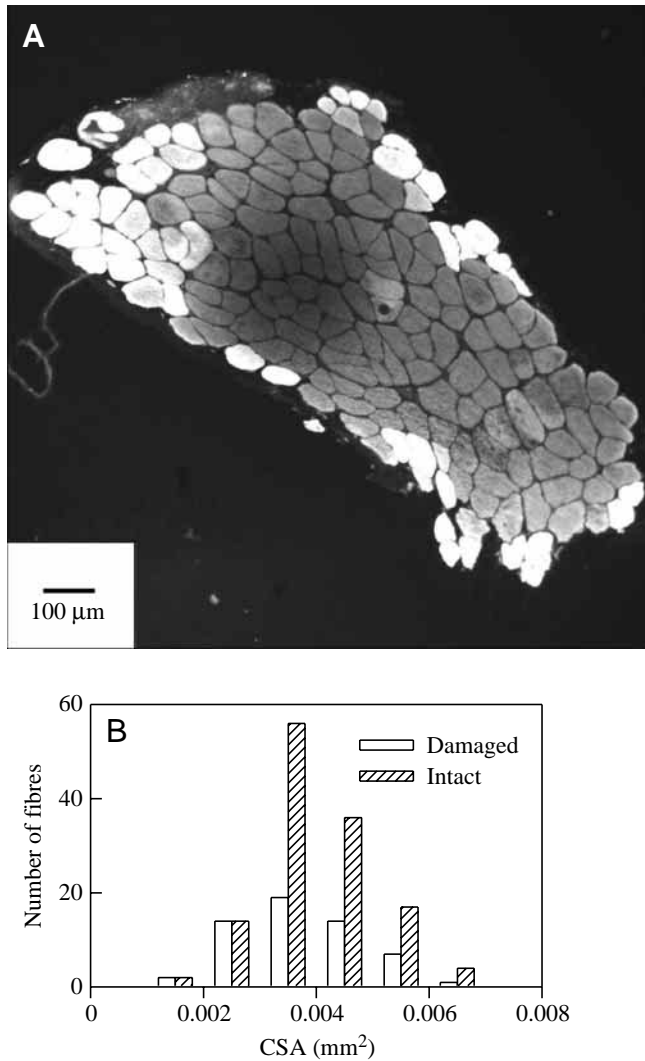


Fig. 1. (A) Video image of a transverse cryo-section of a red fibre bundle after staining with Evans Blue. Intact fibres appear grey and damaged fibres pale. (B) Histogram of the numbers of fibres with different cross-sectional areas (CSA). The muscle preparation was the same as that shown in A.

the damaged fibres are on the surface or clustered near the surface; none is deep within the bundle. To test this further, we calculated the cross-sectional area that would be intact if all the damaged fibres were confined to a continuous layer of fibres at the surface of the bundle. For this calculation, we assumed that fibre diameter was uniform at 81.1 μm (based on the median value for intact fibres, see above). The total area of intact fibres and total area of damaged fibres were calculated for two conditions: one layer of damaged fibres and two layers of damaged fibres. Fig. 2 shows the area of the intact fibres expressed as a fraction of the total area (intact + damaged fibres) for a range of bundle sizes covering that used in the histology experiments. The observations from the histology experiments are also shown; they match the prediction based on one layer of damaged fibres much better than that for two

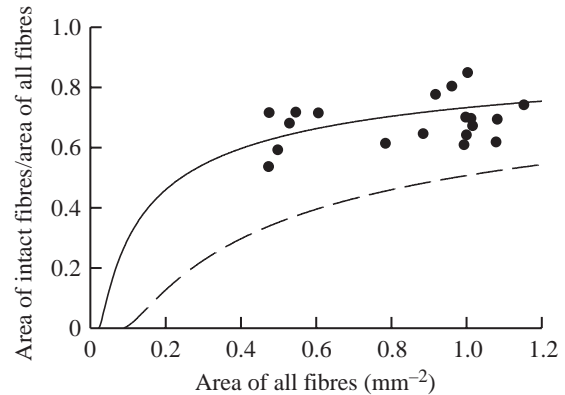


Fig. 2. Relationship between cross-sectional area of intact red fibres expressed as a fraction of total fibre area (intact+damaged) and the area of all fibres. The points are the observed values. The lines were calculated using the following equation on the assumption that damaged fibres were confined at a layer of either one (solid line) or two (broken line) fibres on the surface of the bundle and that the bundle is circular in cross section:  $l/A = [(4A/\pi)^{0.5} - 2d]^2 \pi / (4A)$ , where  $l$  is the area of intact fibres,  $A$  is the area of all fibres (intact+damaged) and  $d$  is the thickness of the layer of damaged fibres. The solid line was calculated using  $d=81.1 \mu\text{m}$ , which is the median fibre diameter measured here (see text), and the broken line assuming that the damaged layer is two fibres thick, i.e.  $d=162.2 \mu\text{m}$ .

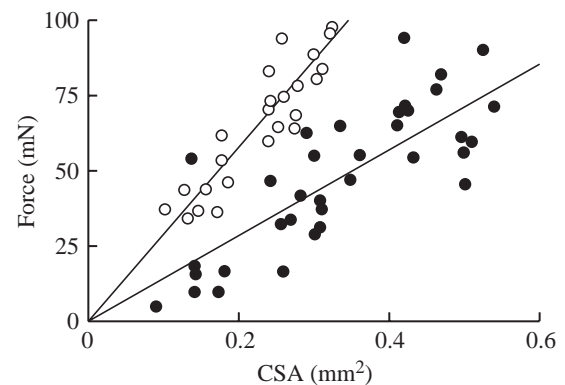


Fig. 3. Relationship between maximum tetanic force and cross-sectional area (CSA) of intact fibres in red (filled symbols) and white (open symbols) muscle preparations. Damaged fibres were removed as described in the text before CSA was measured. The slopes of the lines are the mean of the force/CSA values,  $142.4 \pm 10.3 \text{ kN m}^{-2}$  ( $N=35$ ) for red fibres and  $289.2 \pm 8.4 \text{ kN m}^{-2}$  (means  $\pm$  S.E.M.,  $N=25$ ) for white fibres.

layers of damaged fibres. These results support the idea that most damaged fibres are on the surface of the bundle and that the fraction of the total area that is therefore intact increases with total area in a non-linear manner.

*Isometric force and area of red and white fibre bundles*  
The relationship between maximum isometric force at  $L_0$

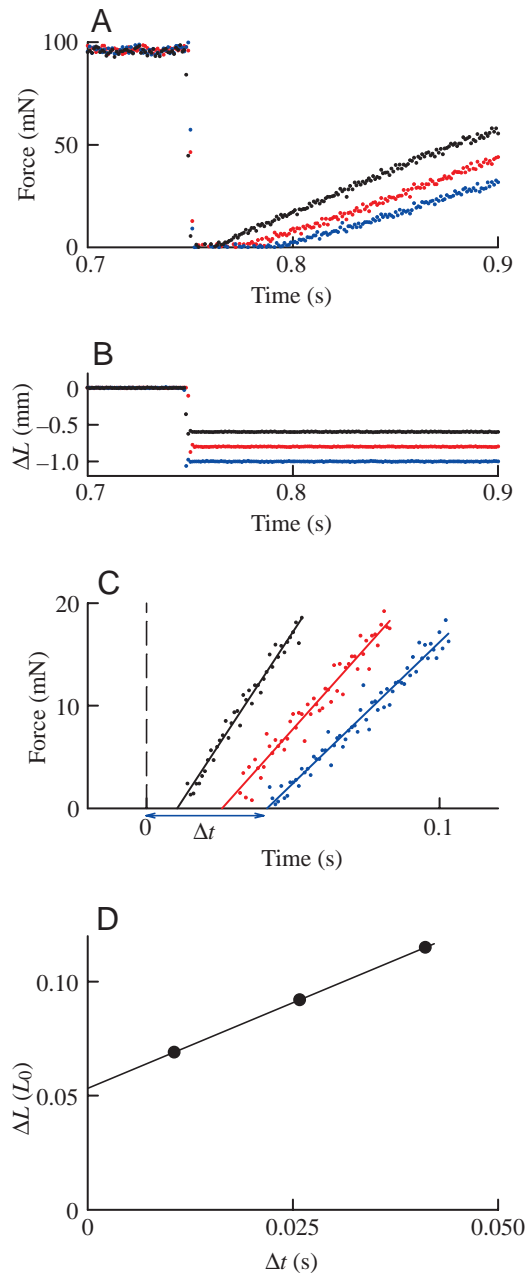


Fig. 4. Sample recordings from the slack test measurements of  $V_0$ , the unloaded velocity of shortening from a red muscle preparation. (A) Three superimposed recordings of tetanic force before and after the length steps ( $\Delta L$ ) shown in B. The fibre bundle was released by different distances from the same starting length. (C) Recordings of force from A shown on expanded scales and with regression lines fitted to the early part of the force redevelopment. The broken vertical lines marks the time of the release. The horizontal arrow marks  $\Delta t$ , the time from the release to the regression intercept for the largest step. This is the time required to take up the slack following the length step. (D) Relationship between step size,  $\Delta L$ , and  $\Delta t$ . The slope of the regression line,  $1.503 \pm 0.002 L_0 s^{-1}$  (mean  $\pm$  s.e.m.,  $N=3$ ), is  $V_0$  for this fibre bundle. The intercept on the  $\Delta L$  axis,  $0.053 \pm 0.0001 L_0$  (mean  $\pm$  s.e.m.  $N=3$ ), is an estimate of the compliance of the series elastic component (SEC) of this fibre bundle.  $L_0$ , the fibre length at which maximum isometric force was produced, was 8.7 mm.

and the cross-sectional area (based on intact fibres) of red and white fibres is shown in Fig. 3. For red fibre bundles, the force per cross-sectional area (stress) was  $142.4 \pm 10.3 \text{ kN m}^{-2}$  ( $N=35$ ). For white fibre bundles, it was considerably greater,  $289.2 \pm 8.4 \text{ kN m}^{-2}$  ( $N=25$ ).

#### $V_0$ for red fibre bundles

Fig. 4 shows sample recordings from the slack test measurement of  $V_0$  (Edman, 1979). The recordings of force after release are shown on an expanded time scale in Fig. 4C with straight lines fitted through the early part of force recovery. The fitted line was extrapolated to the time axis to give a value for the time interval from the step to the start of force recovery. Fig. 4D shows these times *versus* the size of the release. The slope is  $V_0$ , the velocity of shortening under zero load, and the intercept is the amount of shortening by the series elastic component (SEC) during the step itself. For this bundle,  $V_0$  was  $1.503 L_0 s^{-1}$  and the SEC shortening was  $0.053 L_0$ . The mean value of unloaded shortening velocity from six muscle preparations was  $1.693 \pm 0.108 L_0 s^{-1}$  and SEC shortening was  $0.067 \pm 0.006 L_0$ .

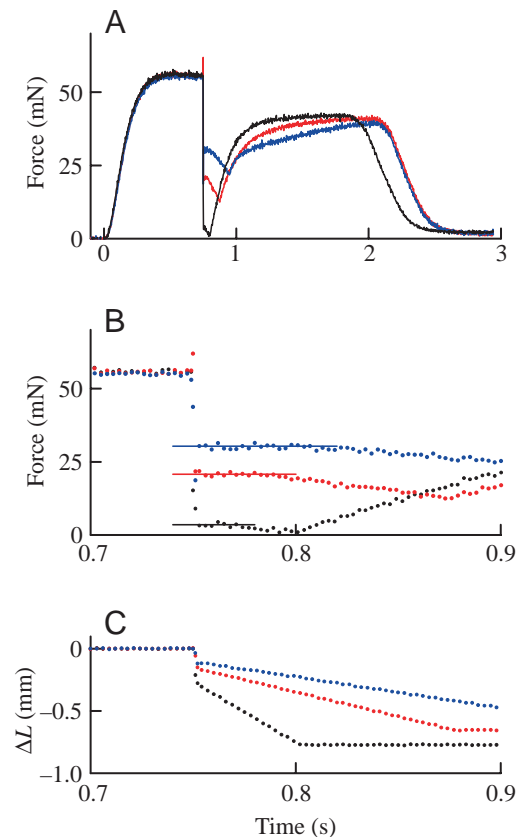


Fig. 5. (A) Three superimposed recordings of active force during tetanic stimulation of a red fibre bundle shortening at different velocities. (B,C) Force and length change ( $\Delta L$ ) on an expanded time scale. The horizontal lines in B show the forces that were measured during the period at the start of the ramp shortening when force was relatively constant.  $L_0$ , the fibre length at which maximum isometric force was produced, was 6.6 mm.

*Force/velocity relationship for red fibre bundles**Shortening*

Fig. 5A shows three superimposed recordings of active force for different step sizes and velocities of ramp shortening. Fig. 5B,C shows the force and length changes on an expanded time scale. On each force recording, a horizontal line shows the value that was measured. This is the force produced by the contractile element as it shortens at constant

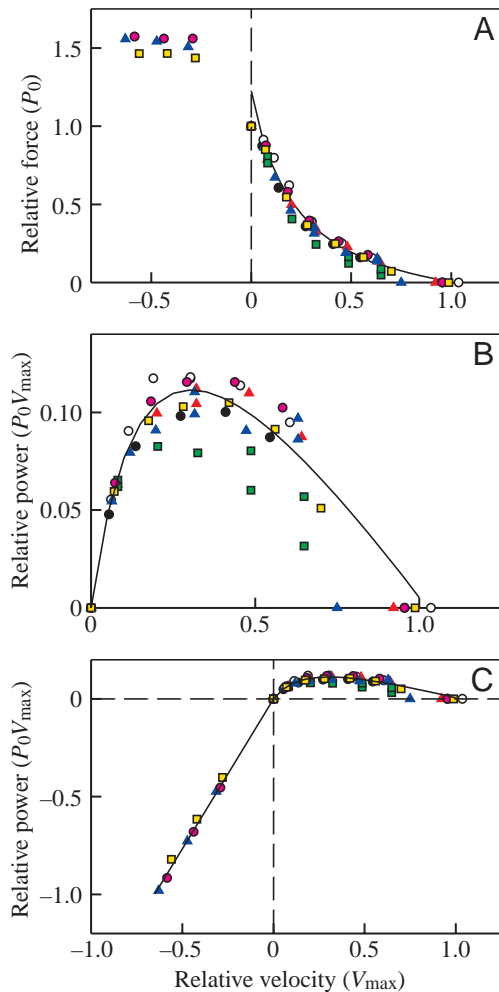


Fig. 6. (A) Summary of the force/velocity results for the seven red fibre bundles (different symbols for different bundles). Force is expressed relative to  $P_0$ , the isometric force at  $L_0$ , the fibre length at which maximum isometric force was produced, and velocity is expressed relative to maximum shortening velocity  $V_{max}$ . Each fibre bundle's values are expressed relative to its own  $P_0$  and  $V_{max}$ .  $V_{max}$  was found for each fibre bundle by fitting a hyperbola to its force/velocity data as described in the text. The line is the mean of these fitted lines for the seven fibre bundles. (B) The relationship between power and velocity of shortening. The points are the products of the force and velocity values shown in A and the line is the mean of the calculated power curves for the seven fibre bundles. (C) The power for both stretch and shortening. The points are the products of the force and velocity values shown in A. The line for shortening is the same as in B. The line for stretch is a straight line fitted through the points and constrained to pass through the origin.

velocity and by the SEC at the length to which it was released during the step. The length of the SEC is constant when force is constant.

For all seven fibre bundles, the relationship between force and the velocity of shortening was hyperbolic, and Hill's equation was fitted for each fibre bundle as described in Materials and methods. The mean values of the fitted parameters, expressed in various units, are included in Table 3A. Fig. 6A shows the results for all the fibre bundles; each fibre bundle's force is expressed relative to its own isometric force at  $L_0$ , and velocity is expressed relative to its own fitted  $V_{max}$ . Note that the isometric force,  $P/P_0=1.0$ , is considerably less than  $P_0^*/P_0$ , the intercept of the fitted line on the force axis. The line in Fig. 6A is the average of the fitted lines for the seven fibre bundles.

Fig. 6B shows the power during shortening, which was calculated as the product of force and the velocity values shown in Fig. 6A. The line in Fig. 6B is the average of the power for the seven fibre bundles, where power was calculated for each bundle from its fitted force/velocity curve. Table 1 lists the maximum power values found in this way.

*Stiffness and compliance of the series elasticity*

Fig. 7A,B shows the characteristics of the SEC of one fibre bundle. The lines were fitted through the points as described in the Materials and methods section (Fig. 7A). The total strain was calculated as if it were due to two structures acting in series: a linear compliance (red line) and another more compliant element with a limited strain range (green line). The results are also plotted as stress *versus* strain in Fig. 7B, showing the typical relationship for a tendon-like structure; the stiffness is low at small stresses and increases to a constant value at higher stresses. For the example shown in Fig. 7, the stiffness of the steep part of the curve was  $26.2[(\Delta P/P_0)/(\Delta L/L_0)]$  [compliance  $0.038(\Delta L/L_0)/(\Delta P/P_0)$ ] and

Table 1. Maximum power output for red fibres

Maximum power	
( $P_0 V_{max}$ )	$0.107 \pm 0.005$
( $W kg^{-1}$ )	$27.4 \pm 1.3$
Velocity	
( $V_{max}$ )	$0.297 \pm 0.012$
( $L_0 s^{-1}$ )	$0.538 \pm 0.028$
Force	
( $P_0$ )	$0.367 \pm 0.010$
( $kN m^{-2}$ )	$52.0 \pm 1.5$

Maximum power was calculated for each fibre bundle from its fitted force/velocity line (power=force  $\times$  velocity).

The mean and S.E.M. for the seven fibre bundles are given, together with the velocity and force at which maximum power was produced.

$P_0$  is the maximum isometric force, which is produced at fibre length  $L_0$ .  $V_{max}$  is the maximum velocity of shortening, which is the intercept between the fitted force/velocity curve and the velocity axis.

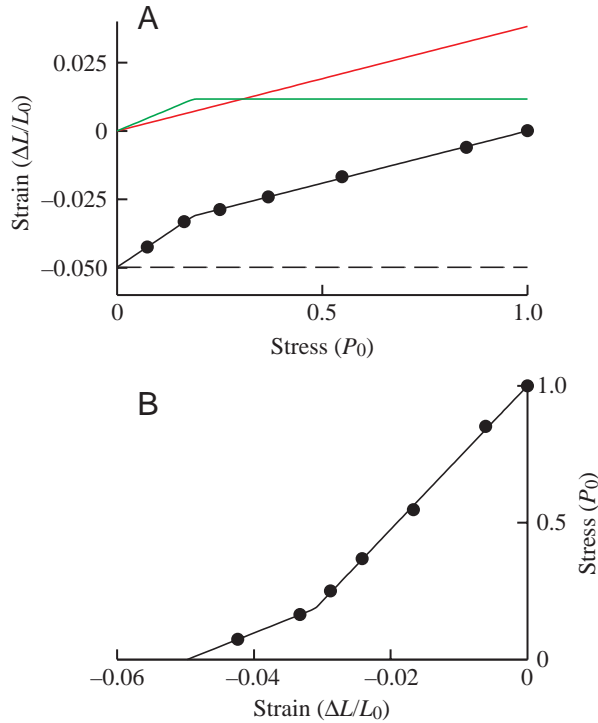


Fig. 7. (A) Example of a stress *versus* strain relationship for the series elastic component of a red fibre bundle. The points show observations from recordings such as those shown in Fig. 5. Stress is that produced at the end of the step change in length, and strain is the size of the step change in length. The fitted line was calculated as described in the text. Strain,  $Y$ , is the sum of a constant,  $k$ , a linear component,  $a(x)$ , and a saturating component,  $b(x)$ , where  $x$  is stress.  $Y=k+a(x)+b(x)$ , where  $a(x)=mx$ ; if  $x < c$ , then  $b(x)=nx$ ; if  $x \geq c$ , then  $b(x)=nc$ . The fitted values were  $k=-0.0498$ ,  $m=0.0381$ ,  $n=0.0625$  and  $c=0.186$ . The total strain (black line) is the sum of  $k$  (broken line) and  $a(x)$  (red line) and  $b(x)$  (green line). (B) Corresponding strain *versus* stress relationship with points and black line as in A.  $\Delta L$ , length change;  $L_0$ , fibre length at which maximum isometric force was produced;  $P_0$ , isometric force before shortening.

Table 2. Characteristics of the series elastic component

High-stiffness region	
Stiffness $(\Delta P/P_0)/(\Delta L/L_0)$	28.3±1.5
Compliance $(\Delta L/L_0)/(\Delta P/P_0)$	0.036±0.002
Low-stiffness region	
Stiffness $(\Delta P/P_0)/(\Delta L/L_0)$	9.68±0.89
Compliance $(\Delta L/L_0)/(\Delta P/P_0)$	0.108±0.010
Intercept ( $L_0$ )	-0.050±0.003

Values are means  $\pm$  S.E.M.,  $N=7$  fibre bundles.

Values of stiffness and compliance are from the two regions of the stress/strain curves for the series elastic component of the fibre bundles.

Intercept is the amount of shortening that reduced stress from  $P_0$  to zero, where  $P_0$  is the maximum isometric force, which is produced at fibre length  $L_0$ . See Fig. 7 and text.

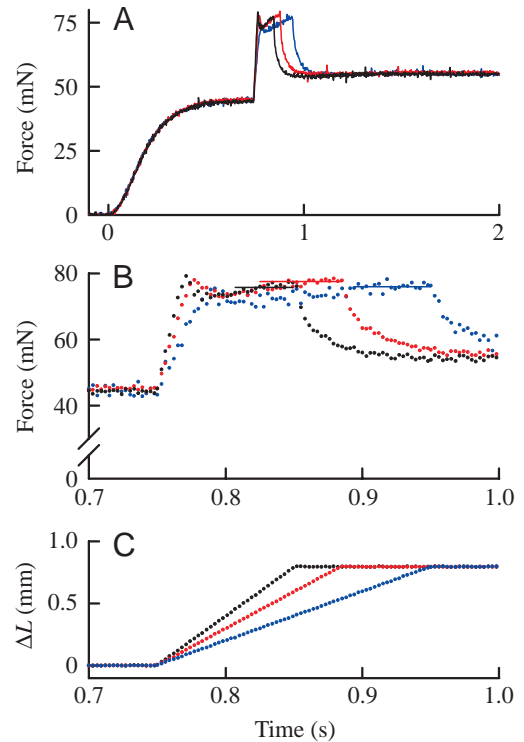


Fig. 8. (A) Three superimposed recordings of active force during tetanic stimulation of a red fibre bundle with stretch at different velocities. (B,C) Force and length change ( $\Delta L$ ) on expanded scales. The horizontal lines in B show the forces that were measured during stretch. Results from the same fibre bundle as in Fig. 5.  $L_0$ , the fibre length at which maximum isometric force was produced, was 6.6 mm.

the stiffness in the less steep part was  $9.94[(\Delta P/P_0)/(\Delta L/L_0)]$  [compliance  $0.101(\Delta L/L_0)/(\Delta P/P_0)$ ]. The size of step required to remove completely the strain produced by stress equal to the isometric force was  $0.050L_0$ , which is the intercept of the fitted line on the strain axis. Similar results were obtained for the seven fibre bundles used in the force/velocity experiments, and the mean values are given in Table 2.

### Stretch

In three of the experiments, the fibre bundle was stretched at a constant velocity to investigate the negative velocity part of the force/velocity relationship. Fig. 8A shows three superimposed recordings for different velocities of stretch. Fig. 8B,C shows the force and length changes on an expanded time scale. On each force recording, a horizontal line shows the value of force that was measured. The force/velocity results are shown in Fig. 6A. All the velocities were within the range where force is relatively independent of velocity. The mean force was  $1.519 \pm 0.032P_0$  ( $N=3$  fibre bundles) during stretch at velocities in the range  $-0.28$  to  $-0.63V_{\max}$ . The power absorbed by the fibre bundles during stretch is shown in Fig. 6C, where its magnitude can be compared with the power output during shortening.

## Discussion

### How much force can red fibres produce?

Using the methods described here to distinguish intact (=live) from damaged fibres, we obtained a mean value for the isometric tetanic force per cross-sectional area of intact fibres of  $142.4 \pm 10.3 \text{ kN m}^{-2}$  ( $N=35$ ). Curtin and Woledge (1993b) reported a smaller value,  $69.0 \pm 7.8 \text{ kN m}^{-2}$  (mean  $\pm$  S.E.M.,  $N=9$ ), for red fibres, but in that study cross-sectional area included all fibres in the bundle (live+damaged). The ratio of these mean values ( $69/142=0.48$ ) suggests that 48% of the fibres in the bundles used by Curtin and Woledge (1993b) were contributing to the contractile force. The histological results presented here are compatible with this conclusion. When the areas of intact and damaged fibres were measured separately, we found that the area of intact fibres depended on total area as if the damaged fibres formed a single layer on the surface of the bundle (Fig. 2). The mean total bundle area was  $0.310 \pm 0.040 \text{ mm}^2$  (mean  $\pm$  S.E.M.,  $N=9$ ) in our previous study (Curtin and Woledge, 1993b). Assuming that the surface layer of fibres was damaged, intact fibres would have constituted 55% of the total area, which is in reasonably good agreement with the value of 48% expected on the basis of force comparison.

### Are red fibres as strong as white fibres?

Table 3 shows the force per cross-sectional area produced by white fibres from dogfish in experiments in which only live fibres are included in the cross-sectional area. The value,  $289.2 \pm 8.4 \text{ kN m}^{-2}$  ( $N=25$ ), is considerably greater than that produced by intact red fibres,  $142.4 \pm 10.3 \text{ kN m}^{-2}$  ( $N=35$ ).

At least part of the difference between white and red fibres

of dogfish is because a larger fraction of the cross-sectional area consists of myofibrils in white fibres than in red fibres, as discussed by Altringham and Johnston (1982). Bone et al. (1986; their Table 1) found that mitochondria occupy only  $0.99 \pm 0.16\%$  (mean  $\pm$  S.E.M.) of the volume of white fibres, but  $21.55 \pm 3.39\%$  (mean  $\pm$  S.E.M.) of the volume of red fibres in fully grown dogfish (as were used in the present study). These results can be used to express the force relative to the cross-sectional area not occupied by mitochondria. Using this ratio and the isometric force values in Table 3 gives the following values:  $292.1 \text{ kN m}^{-2}$  ( $=289.2/0.99$ ) for white fibres and  $180.2 \text{ kN m}^{-2}$  ( $=142.4/0.79$ ) for intact red fibres. Therefore, the evidence indicates that red fibres are not as strong as white fibres, even after effects due to damaged fibres and the difference in mitochondrial volume have been taken into account.

### Force/velocity characteristics and power output for red fibres Comparison with red fibres from other species of fish

Table 4 summarizes the force/velocity characteristics and maximum power output of red fibres from other species of fish. In all cases, the fish had been acclimated to the temperature at which the acute experiments were carried out. There is a threefold range in maximum power output ( $26.5\text{--}70.9 \text{ W kg}^{-1}$ ), with dogfish and carp (*Cyprinus carpio*) fin muscle producing very similar low values and scup (*Stenotomus chrysops* L.) producing the highest. The low power from dogfish and carp fin muscle reflects their low  $V_{\max}$ . In addition, both muscle have a low value for maximum power, approximately  $0.11 P_0 V_{\max}$ , which indicates that they produce relatively little power given their capacity to produce isometric force and their

Fig. 9. Comparison of the force and power output by intact white (Curtin and Woledge, 1988) and red muscle fibres. Black lines (white fibres) and red lines (red fibres) were calculated from Hill's equation using the mean values of the fitted constants in Table 3A (means for seven white fibre preparations and seven red fibre preparations). (A) The relationship between relative force and relative velocity calculated from the following:  $P' = \{[B(P^*+A)]/(V'+B)\} - A$ , where  $P'$  is force expressed relative to  $P_0$ , the maximum isometric force,  $V'$  is velocity expressed relative to  $V_{\max}$ , the maximum velocity of shortening, which is the intercept of the force/velocity curve on the velocity axis. Table 3A includes the values of the constants:  $P^* = P_0^*/P_0 = 1.228 \pm 0.053$  for red fibres and  $1.19 \pm 0.04$  for white fibres;  $A = a/P_0 = 0.269 \pm 0.024$  for red fibres and  $0.274 \pm 0.020$  for white fibres;  $B = b/V_{\max} = 0.225 \pm 0.024$  for red fibres and  $0.236 \pm 0.022$  for white fibres. (B) The relationship between relative power and relative velocity calculated from the following: relative power  $= P'V'$ , where  $P'$  and  $V'$  are defined as in A. (C,D) The corresponding relationships with force expressed in units of force per cross-sectional area and velocity expressed in units of  $L_0 \text{ s}^{-1}$ , where  $L_0$  is the fibre length at which maximum isometric force,  $P_0$ , was produced.

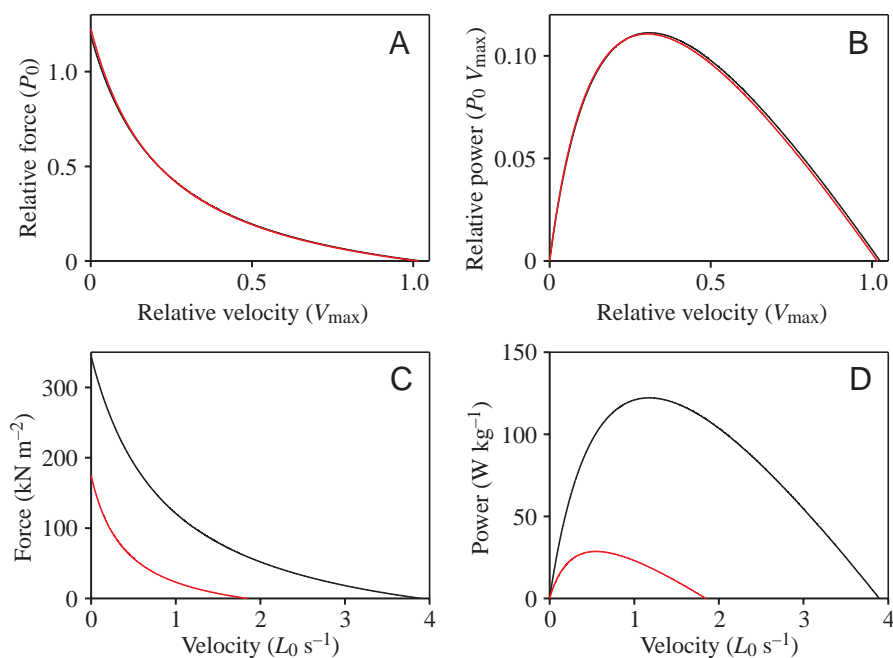




Table 3. Force/velocity characteristics and power from red and white fibres of dogfish

	Red fibres	N	White fibres	N
A Observed $P_0$ and fitted values				
$P_0$ (kN m <sup>-2</sup> )	142.4±10.3	35	289.2±8.4	25
$V_{max}$ (L <sub>0</sub> s <sup>-1</sup> )	1.814±0.071	7	3.8±0.2	13
$a/P_0$	0.269±0.024	7	0.274±0.020	7
$b/V_{max}$	0.225±0.024	7	0.236±0.022	7
$b$ (L <sub>0</sub> s <sup>-1</sup> )	0.404±0.041	7	NA	
$P_0^*/P_0$	1.228±0.053	7	1.19±0.04	7
B Values calculated from observed $P_0$ and fitted values				
Maximum power				
( $P_0V_{max}$ )		0.111±0.111		
At $V/V_{max}$		0.30±0.31		
Maximum power				
(W kg <sup>-1</sup> )		28.6±122.2		
Velocity at maximum power (L <sub>0</sub> s <sup>-1</sup> )		0.544±1.178		

Values are means ± S.E.M.

(A)  $P_0$ , maximum isometric force produced at fibre length  $L_0$  from experiments reported here for red and white fibres.  $V_{max}$  and  $P_0^*$  are the intercepts and  $a$  and  $b$  are the constants found by fitting the hyperbolic Hill relationship to the force/velocity results reported here for red fibres (see text).

Corresponding values for the force/velocity relationship for white fibres are from Curtin and Woledge (1988).

Values that are not available are indicated NA.

(B) Maximum power and velocity and force at maximum power calculated from the values in A.

maximum velocity of shortening. In other words, their force/velocity relationships are more curved than those of carp and scup myotomal muscle. There is no clear pattern in the relationship between isometric force and maximum power output.

Comparison of red and white fibres from dogfish

The results reported here can be used to compare the performance of red and white fibres from the same species of fish. Fig. 9 and Table 3 compare the fitted force/velocity and power/velocity curves for red and white fibres from dogfish. In Fig. 9A,B, force is expressed as a fraction of isometric force and velocity as a fraction of the maximum velocity of shortening to remove variations between these fibre types that are due to differences in intrinsic isometric strength and the maximum velocity of filament sliding. The curves for red and white fibres are very similar. For both fibre types, the maximum power output is 0.111 $P_0V_{max}$  and is produced during shortening at 0.30 $V_{max}$  in red fibres and 0.31 $V_{max}$  in white fibres. In terms of muscle function, this means that the red and white fibres have equal capacities to produce power within the limits set by the isometric force and maximum velocity of shortening of each fibre type.

Fig. 9C shows the force/velocity relationships for red and white fibres calculated from the mean values of the constants found by fitting the hyperbolic Hill equation to the data and the value of  $P_0$  (in kN m<sup>-2</sup>). The isometric force of red fibres is approximately 49% of that for white fibres; the difference in maximum velocity of shortening is very similar, the value for red fibres being 48% of that of white fibres. Fig. 9D shows

Table 4. Comparison of power and force/velocity characteristics for intact red fibres from different fish

	Dogfish		Carp fin		Carp		Scup	
	Mean	N	Mean	N	Mean	N	Mean	N
$P_0$ (kN m <sup>-2</sup> )	142.4±10.3	35	202±8	6	109.1 <sup>1</sup> NA		169 <sup>3</sup> NA	
$V_{max}$ (L <sub>0</sub> s <sup>-1</sup> )	1.814±0.071	7	1.18±0.04	6	3.55±0.16	8	3.32	
Maximum power								
( $P_0V_{max}$ )	0.107±0.005	7	0.11±0.007	6	0.154 <sup>2</sup> NA		0.128±0.005	8
(W kg <sup>-1</sup> )	27.4±1.3	7	26.5 NA		59.7±2.3	6	70.9±8.1	8
Temperature (°C)	12		8		10		10	
Reference	a		b		c		d	

Values are means ± S.E.M.

$P_0$  is the maximum force in an isometric tetanus at  $L_0$ , the fibre length giving maximum isometric force.  $V_{max}$  is the maximum velocity of shortening. Maximum power is the highest power produced during shortening under constant-velocity or constant-force conditions.

Superscripts indicate calculated values: <sup>1</sup>from  $Q_{10}=1.13$  and  $P_0$  at 15 °C in Rome and Sosnicki (1990), <sup>2</sup>from the other values in the column, and <sup>3</sup>from  $Q_{10}=1.08$  and  $P_0$  at 20 °C in Rome et al. (1992).

Values that are not available are indicated NA.

Temperature was the same during acclimation of the fish and during the acute experiment.

References: <sup>a</sup>Present study, Table 1; <sup>b</sup>Langfeld et al. (1991); <sup>c</sup>Rome and Sosnicki (1990); <sup>d</sup>Rome et al. (1992).

the corresponding power/velocity relationships with power (in  $\text{W kg}^{-1}$ ). From the fitted curves, the maximum power output of the red fibres,  $28.6 \text{ W kg}^{-1}$ , is only 23% of that of the white fibres,  $122.2 \text{ W kg}^{-1}$ . Clearly, both the red fibres' lower capacity to produce force and the slower intrinsic velocity of filament sliding contribute to making their power output less than that of white fibres (see Table 3A).

How do these differences in power output of red and white fibres compare with those of mammalian fibres? The dogfish fibres are like mammalian fibre types in that the maximum power output of mouse soleus (red) fibres,  $23.6 \pm 1.8 \text{ W kg}^{-1}$  (mean  $\pm$  S.E.M.,  $N=6$ ), is less than that of mouse extensor digitorum (white) fibres,  $57.2 \pm 4.2 \text{ W kg}^{-1}$  (mean  $\pm$  S.E.M.,  $N=6$ ) (Barclay et al., 1993). However, there is an important difference; whereas dogfish red and white fibre power is the same when expressed relative to  $P_0 V_{\max}$  (see above), in mouse the red fibres' maximum power expressed relative to  $P_0 V_{\max}$  is only 86% of the corresponding value for white fibres (Barclay et al., 1993). Thus, the dogfish red fibres are more effective than mouse red fibres at translating their intrinsic strength ( $P_0$ ) and intrinsic shortening speed ( $V_{\max}$ ) into power output.

#### *Force/velocity relationship during stretch*

We report here that red fibres produce a force of  $1.519 \pm 0.017 P_0$  ( $N=3$ ) during isovelocity stretch. This is very similar to the results of an earlier study of white muscle fibres from dogfish,  $1.569 \pm 0.031 P_0$ , (mean  $\pm$  S.E.M.,  $N=3$ ; see Fig. 1D in Curtin et al., 1998). The velocity ranges used in the two studies were different, but it has been clearly established from many studies of muscle from other species (for example, Aubert, 1956; Lombardi and Piazzesi, 1990) that the force during stretch is independent of velocity except in the very low velocity range. Thus, it seems that red and white fibres of dogfish are very similar both during stretch and during shortening, two conditions in which there are important differences in the cross-bridge cycle (Lombardi and Piazzesi, 1990; Piazzesi and Lombardi, 1995) and energy (Curtin and Davies, 1973) turnover.

#### *Comparison of isovelocity shortening and sinusoidal movement*

Although maximum power output during sinusoidal movement of red fibres has been investigated previously (Curtin and Woledge, 1993b), the value is not comparable with that reported here. In these two studies, different methods were used to normalize for the amount of live fibre in the preparation (maximum rate of energy output and mass of live fibres) and, consequently, maximum power is reported in different units. However, it is possible to compare the velocities of movement at which power was maximal. In the experiments reported here on fully active red fibres, maximum power was produced during isovelocity shortening at  $0.3 V_{\max}$ , which is equivalent to  $0.544 L_0 s^{-1}$  (Table 3). This can be compared with maximum power output during sinusoidal movement, which resembles that during swimming. Power output has been measured at

movement frequencies in the range 0.61–1.67 Hz with a stimulus duty cycle of 0.3. The stimulus phase was optimized to give maximum power at each movement frequency. Maximum power output occurred at a movement frequency of  $1.02 \pm 0.066 \text{ Hz}$  ( $N=9$ ). At this frequency, the maximum instantaneous velocity was  $0.31 L_0 s^{-1}$  and the mean velocity was  $0.147 L_0 s^{-1}$ ; both are considerably lower than the velocity ( $0.544 L_0 s^{-1}$ ) giving maximum power during isovelocity shortening of fully active red fibres. This difference is probably due to the time required for the relatively slow rise in force and, perhaps more importantly, the slow relaxation of force in the sinusoidal experiments, where stimulation is intermittent. If relaxation of force is not completed during the shortening part of the sinusoidal movement, this results in negative power during stretch and a reduction in the net power for the complete cycle of movement.

#### *Stress/strain characteristics of the series elastic component*

There is reasonable agreement between the two estimates of the size of release required to reduce isometric force to zero. The slack test experiments gave a mean value of  $0.067 \pm 0.006 L_0$  ( $N=6$ ) and the value from the force/velocity experiments (Fig. 7) is  $0.050 \pm 0.003 L_0$  ( $N=7$ ).

As stated in the Results, the shape of the stress/strain curve shown in Fig. 7B is typical for tendon (Ker et al., 1986; Alexander, 1988) in that stiffness is low at small stresses and increases to a constant value at higher stresses. The stiffness of the steep part of the curve is 4.09 MPa, which is considerably less than that expected for tendon, approximately 1500 MPa (Alexander, 1988). However, a large discrepancy is expected because our value uses the stress expressed as force per cross-sectional area of the muscle fibres, an area that is much larger than the cross-sectional area of the pieces of myosepta. It is also relevant that, although the myosepta are the major determinant of the observed stiffness, other structures in addition to the myosepta are likely to contribute to the elastic characteristics we measure. These structures include the thick and thin contractile filaments within the muscle fibres themselves, which act in series with the cross-bridges to transmit force to the ends of the fibres.

We thank Dr G. Coulton for help with the image analysis and Mrs Allia Syed for technical assistance. The Biotechnology and Biological Sciences Research Council (UK) supported this work.

#### References

- Alexander, R. McN. (1988). *Elastic Mechanisms in Animal Movement*. Cambridge: Cambridge University Press.
- Altringham, J. D. and Johnston, I. A. (1982). The pCa-tension and force-velocity characteristics of skinned fibres isolated from fish fast and slow muscles. *J. Physiol., Lond.* **333**, 421–449.
- Aubert, X. (1956). *Le Couplage Energetique de la Contraction Musculaire*. Brussels: Arscia.
- Barclay, C. J., Constable, J. K. and Gibbs, C. L. (1993). Energetics of fast- and slow-twitch muscle of the mouse. *J. Physiol., Lond.* **472**, 61–80.

- Bone, Q.** (1966). On the function of the two types of myotomal muscle fibre in elasmobranch fish. *J. Mar. Biol. Ass. UK* **46**, 321–349.
- Bone, Q., Johnston, I. A., Pulsford, A. and Ryan, K. P.** (1986). Contractile properties and ultrastructure of three types of muscle fibre in the dogfish myotome. *J. Muscle Res. Cell Motil.* **7**, 47–56.
- Curtin, N. A. and Davies, R. E.** (1973). Chemical and mechanical changes during stretching of activated frog skeletal muscle. *Cold Spring Harbor Symp. Quant. Biol.* **37**, 619–626.
- Curtin, N. A., Gardner-Medwin, A. R. and Woledge, R. C.** (1998). Predictions of the time-course of force and power output by dogfish white muscle fibres during brief tetani. *J. Exp. Biol.* **201**, 103–114.
- Curtin, N. A. and Woledge, R. C.** (1988). Power output and force/velocity relationship of live fibres from white myotomal muscle of the dogfish *Scyliorhinus canicula*. *J. Exp. Biol.* **140**, 187–197.
- Curtin, N. A. and Woledge, R. C.** (1993a). Efficiency of energy conversion during sinusoidal movement of white muscle fibres from the dogfish *Scyliorhinus canicula*. *J. Exp. Biol.* **183**, 137–147.
- Curtin, N. A. and Woledge, R. C.** (1993b). Efficiency of energy conversion during sinusoidal movement of red muscle fibres from the dogfish *Scyliorhinus canicula*. *J. Exp. Biol.* **185**, 195–206.
- Edman, K. A. P.** (1979). The velocity of unloaded shortening and its relation to sarcomere length and isometric force in vertebrate muscle fibres. *J. Physiol., Lond.* **291**, 143–159.
- Hill, A. V.** (1938). The heat of shortening and the dynamic constants of muscle. *Proc. R. Soc. B* **126**, 136–195.
- Ker, R. F., Dimery, N. J. and Alexander, R. McN.** (1986). The role of tendon elasticity in hopping in a wallaby (*Macropus rufogriseus*). *J. Zool., Lond. A* **208**, 417–428.
- Langfeld, K. S., Crockford, T. and Johnston, I. A.** (1991). Temperature acclimation in the common carp: force–velocity characteristics of myosin subunit composition of slow muscle fibres. *J. Exp. Biol.* **155**, 291–304.
- Lombardi, V. and Piazzesi, G.** (1990). The contractile response during steady lengthening of stimulated frog muscle fibres. *J. Physiol., Lond.* **431**, 141–171.
- Piazzesi, G. and Lombardi, V.** (1995). A cross-bridge model that is able to explain mechanical and energetic properties of shortening muscle. *Biophys. J.* **68**, 1966–1979.
- Rome, L. C. and Sosnicki, A. A.** (1990). The influence of temperature on mechanics of red muscle in carp. *J. Physiol., Lond.* **427**, 151–169.
- Rome, L. C., Sosnicki, A. and Choi, I.-H.** (1992). The influence of temperature on muscle function in the fast-swimming scup. II. The mechanics of red muscle. *J. Exp. Biol.* **163**, 281–295.